

Comparison of measured and simulated parallel flows at the edge plasma of MAST

P. Molchanov^a, V. Rozhansky^a, S. Voskoboynikov^a, S. Tallents^b

G. Counsell^c, A. Kirk^c

^a*St.Petersburg State Polytechnical University, Polytechnicheskaya 29, St.Petersburg, Russia*

^b*Imperial College, Prince Consort Road, London SW7 2BZ, UK*

^c*EURATOM/UKAEA Fusion Association, Culham Science Centre, Abingdon, Oxon, OX14 3DB, UK*

Abstract

A comparison is presented of measured and simulated parallel flows in the low field side scrape-off layer of MAST Ohmic shots. Simulations with B2SOLPS5.0 code reproduce the experimentally observed co-current rotation direction. The absolute values of the simulated Mach number are smaller than those of the measured ones; the difference might reach a factor of two. It is demonstrated that in both the simulations and the experiment the parallel velocity increases with temperature and decreases with poloidal magnetic field.

1. Introduction

Parallel velocity at the edge plasma has been measured using Mach probes for various tokamaks: JET [1], ASDEX Upgrade [2]-[3], Alcator C-MOD [4], TCV [5], JT-60 [6] and others, see also references in [7]. There were also several simulations of the parallel flows in the scrape-off layer (SOL) performed using the fluid codes EDGE2D [8], UEDGE [9], B2SOLPS5.0 [10]-[11]. The Mach numbers obtained in the simulations are usually of the same order as measured in the experiments but are smaller by a factor 1-3.

As was demonstrated in [10], results of simulations of parallel flows in the SOL's of ASDEX Upgrade and MAST Ohmic shots are consistent qualitatively with a simple analytical expression for Pfirsch-Schlueter flows and flows compensating $\vec{E} \times \vec{B}$ drifts. The physics of these flows has been discussed in [12] and references therein. In particular, the T/B_x parametric dependence (T is the SOL temperature, B_x is the SOL poloidal magnetic field)

has been observed in the simulations [10]. It was also found that the density and toroidal magnetic field dependence is rather weak for these flows.

In the simulations reported in [10], the parametric scan was performed with other parameters being constant. In real Ohmic shots, however, the density rise would cause a simultaneous temperature drop, the tokamak current rise could cause a temperature rise etc. The aim of this paper is to simulate real MAST Ohmic discharges with varying density and plasma current designed to explore the parameter space in a systematic fashion, and to perform a comparison of the simulation results with the Mach probe measurements for these shots, and to check the predicted T/B_x parametric dependence for the parallel SOL flows.

2. Experimental data

Data presented are from a series of discharges undertaken as a preliminary investigation, and a further campaign based on three repeatable scenarios systematically exploring the parameter space. Multiple discharges of each scenario type were performed to provide sufficient data for analysis over the entire SOL. These scenarios were designed to use density (to which the flow is predicted to be insensitive) to compensate for changes in the plasma current, thus providing flow data from: high poloidal field and low temperature discharges (based on shot № 16290); high poloidal field and high temperature discharges (based on shot № 17825); and low poloidal field and low temperature discharges (based on shot № 17838).

Mach numbers were measured at the outboard mid-plane of MAST using two diametrically-opposite, field-aligned pins on the MAST Gundestrup probe, driven into ion saturation current mode by 200V, 3A power supplies. This constitutes a Mach probe [13], with the Mach number calculated using the Hutchinson formula [14] in the usual way.

3. Simulations results

Five Ohmic shots have been chosen for simulations, the global parameters are shown in Table 1. In the simulations the following boundary conditions at the core side of the simulation domain (4-5cm inside the separatrix at the equatorial mid-plane for shots №16290, №17838, №17825 and 10cm for shots №15214, №15226) were chosen. Shot №16290: $n_e|_{core} = 1.3 \times 10^{19} m^{-3}$, $T_e|_{core} = T_i|_{core} = 60eV$, shot №17838: $n_e|_{core} = 6.3 \times 10^{18} m^{-3}$, $T_e|_{core} = T_i|_{core} = 110eV$, shot №17825: $n_e|_{core} = 5.6 \times 10^{18} m^{-3}$, $T_e|_{core} = T_i|_{core} = 88eV$, shot

$$\begin{aligned} \text{№15214: } n_e|_{core} &= 1.75 \times 10^{18} m^{-3}, & T_e|_{core} &= T_i|_{core} = 210 eV, & \text{shot } \text{№15226:} \\ n_e|_{core} &= 1.75 \times 10^{18} m^{-3} & T_e|_{core} &= T_i|_{core} = 107 eV. \end{aligned}$$

In all discharges co-current (negative) parallel velocity has been obtained both in the experiments and simulations. The measurements were made at the LFS equatorial mid-plane. The group of Mach probe measurements is shown in Fig.1. In this group of shots the variation in poloidal magnetic field was rather weak ($\sim 15\%$). The density variation was of the order of 50%. For simulations, two shots with almost the same density but different temperatures have been chosen, to study the temperature dependence of the parallel flow.

The second group of simulation results and measurements are shown in Figs. 2-4. Here both density and temperature varied.

4. Discussion

Both simulations and measurements give co-current parallel velocity in the SOL. The Mach number defined as

$$M = \frac{|V_{\parallel}|}{\sqrt{(T_e + T_i)/m_i}} \quad (1)$$

is smaller in the simulations than the measured one, the difference is up to a factor of 2. This situation is also typical for other tokamaks [8]-[11].

In [10] it was demonstrated that the parametric dependence of the simulation results is consistent with the simple model expression

$$V_{\parallel}^{MODEL} = V_{\parallel}^{PS} + V_{\parallel}^E, \quad (2)$$

where

$$V_{\parallel}^{P.S.} = \left(\frac{1}{en_e h_y} \frac{\partial p_i}{\partial y} + \frac{1}{h_y} \frac{\partial \varphi}{\partial y} \right) \frac{B_z}{B_x B} \left(1 - \frac{B^2}{\langle B^2 \rangle} \right), \quad (3)$$

$$V_{\parallel}^E = \frac{1}{B_x} \frac{\partial \phi}{h_y \partial y}. \quad (4)$$

Here $\partial/h_y \partial y$ is the radial (normal to the flux surface) derivative, B_x , B_z and B are poloidal, toroidal and total magnetic fields, p_i is the ion pressure, ϕ is the electrostatic potential. The first part of the parallel velocity is the Pfirsch-Schlueter velocity, calculated under the assumption that p_i and ϕ are flux surface quantities. The second part is the velocity compensating the poloidal $\vec{E} \times \vec{B}$ drift in the radial electric field. Note that these are simplified expressions, in particular assumptions $p_i = \text{const}$, $\phi = \text{const}$ are not fulfilled in the SOL. Moreover, an additional parallel flux caused by the inner-outer diverter asymmetries, which is not directly connected with electric and diamagnetic drifts, should be added to Eq. (2). However, as was shown in [10], the parallel velocity from Eq. (2) is similar to that obtained in the simulations and has the same parametric dependence.

The parallel velocity calculated according to Eq. (2) is also plotted in Figs. 2-4. As can be seen in the SOL 2-3cm outside the separatrix, analytical, simulations by the B2SOLPS5.0 code and measured parallel velocities are of the same order for all this shots. The possible exception is the shot shown in Fig.2 where a factor of two difference is found.

On the basis of Eq. (2) one would expect the following parametric dependence of the parallel velocity in the SOL

$$V_{\parallel} = A \frac{T}{B_x}, \quad (5)$$

where A is some coefficient, B_x is the local poloidal magnetic field and T is the SOL temperature (this is the average of the electron and ion temperatures in the SOL, because $T_i \sim T_e$ is assumed in the derivation of this scaling law) taken locally at the outer mid-plane. This scaling could be obtained from Eq. (2) assuming constant SOL width, $\phi \sim T_e/e$ and $T_i \sim T_e$. No strong density or toroidal magnetic field dependence is expected.

The temperature dependence of the Mach number measured for the shots shown in Fig.1 is qualitatively consistent with the scaling: larger Mach numbers corresponds to larger SOL temperatures. In Fig. 5 the Mach number at a reference point (defined as 3cm outside the separatrix at the LFS mid-plane) is plotted versus T/B_x for shots №16290, №17838,

№17825. To calculate the absolute values of the parallel velocity the Mach number should be multiplied by the sound speed. Since the ion temperature was not measured, the simulated ion and electron temperatures were used to calculate the sound speed. The absolute value of the parallel velocity at the reference point is shown in Fig. 6. One can see that an approximately linear rise with the parameter T/B_x is observed both for experimental and simulated velocities in accordance with the scaling Eq. (5).

In Figs. 7-8 the absolute value of the parallel velocity is plotted versus local values of the parameter T/B_x taken locally at the equatorial mid-plane for distances in the range 1-5 cm outside the separatrix. The shots №15214, №15226 were not included in this plot because they were simulated in similar, but not real geometry and some parameters may not be consistent with the real discharges (especially profiles of T/B_x). Again the dependence may be approximated as linear one in both the experiment and modeling.

3. Conclusions

Simulations with the B2SOLPS5.0 code reproduce the experimentally observed co-current rotation direction in the low field side scrape-off layer in Ohmic shots of MAST. The absolute values of the simulated Mach number are smaller than those of the measured ones; the difference is up to a factor of two. The simple analytical expression, Eqs. (2)-(4), is consistent with the measurements and simulations. The parallel velocity is increasing with temperature and decreasing with poloidal magnetic field as suggested by the scaling Eq. (5).

References

1. Erents S K et al Plasma Phys. Control. Fusion 46 (2004) 1757
2. Muller H W et al Proc. 32 EPS Conf. Plasma Phys. Contr. Fus. Tarragona (2005) P-1.009
3. Muller H W et al Journal of Nuclear Materials 363-365 (2007) 664
4. Labombard B et al Nuclear Fusion 44 (2004) 1047
5. Pitts R A et al Journal of Nuclear Materials 363-365 (2007) 575
6. Asakura N et al Nuclear Fusion 44 (2004) 503

7. Asakura N Journal of Nuclear Materials 363-365 (2007) 41
8. Chankin A V, Corrigan G, Erements S K Journal of Nuclear Materials 290-293 (2001) 518
9. Porter G D, Ronglien T D, Rensink M E Journal of Nuclear Materials 313-316 (2003) 1085
10. Rozhansky V et al Journal of Nuclear Materials 363-365 (2007) 605
11. Hoshino K et al Journal of Nuclear Materials 363-365 (2007) 539
12. Rozhansky V Contrib. Plasma Phys. 46 (2006) 575
13. Matthews G F Plasma Phys. Control. Fusion 36 (1994) 1595
14. Hutchinson I H Physical Review A 37 (1988) 4358

Table 1. Global plasma parameters. Here T_{e0} and n_{e0} are central electron temperature and density, Wp is the plasma stored energy, I_p is the plasma current, B_z is the toroidal magnetic field, P_{ohmic} is the Ohmic power.

Shot	T_{e0} [eV]	n_{e0} [$10^{19}m^{-3}$]	Wp [kJ]	I_p [MA]	B_z [T]	P_{ohmic} [MW]
15214	750	2.7	8	0.8	0.5	1.8
15226	700	3.0	10	0.5	0.5	1.1
16290	700	3.8	9.5	0.7	0.5	1.3
17825	680	2.3	9	0.4	0.5	0.5
17838	1000	2.5	11.5	0.7	0.6	0.9

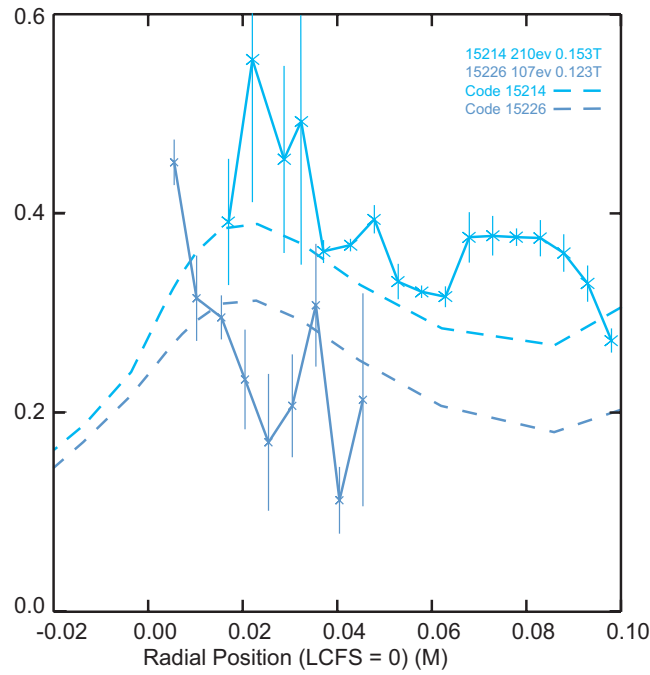


Fig.1. Mach number radial profiles at the outer mid-plane (temperature scan). The radial coordinate is the distance from the LCFS; positive values correspond to the SOL, negative – to the core region.

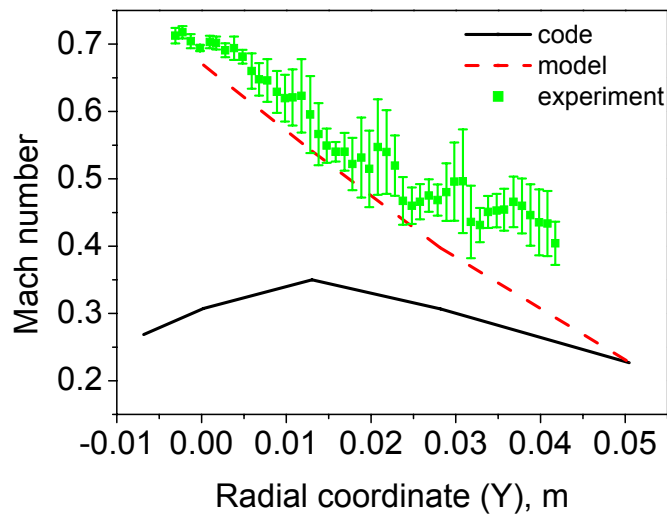


Fig.2. Mach number radial profiles at the outer mid-plane for the scenario based on shot №17825 with low plasma current and low density.

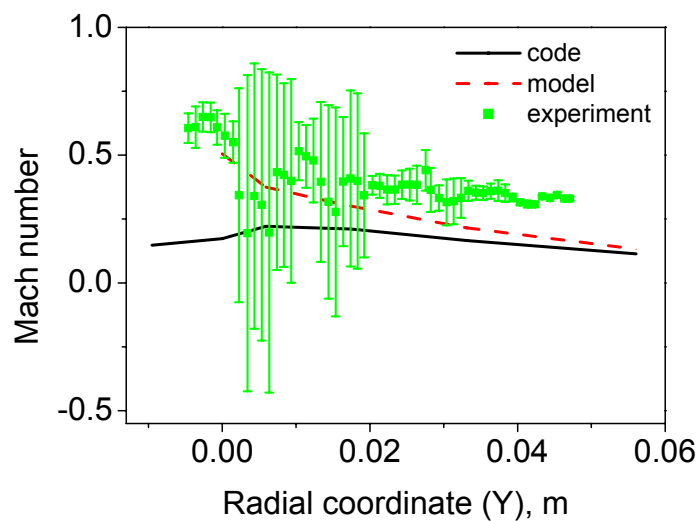


Fig.3. Mach number radial profiles at the outer mid-plane for the scenario based on shot №17838 with high plasma current and low density.

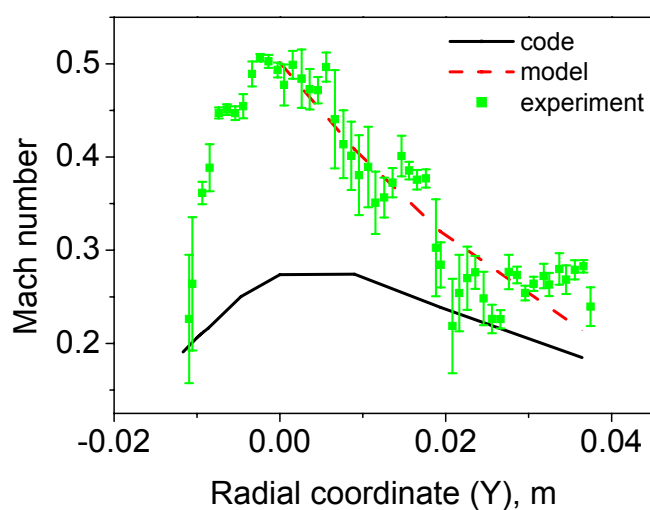


Fig.4. Mach number radial profiles at the outer mid-plane for the scenario based on shot №16290 with high plasma current and high density.

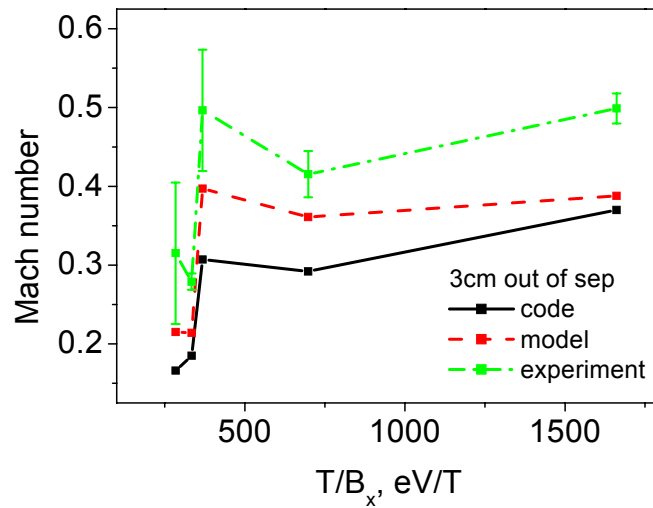


Fig.5. Mach number at the reference point in the equatorial mid-plane 3 cm outside the separatrix as a function of the ratio of the SOL temperature to poloidal magnetic field for all scenarios.

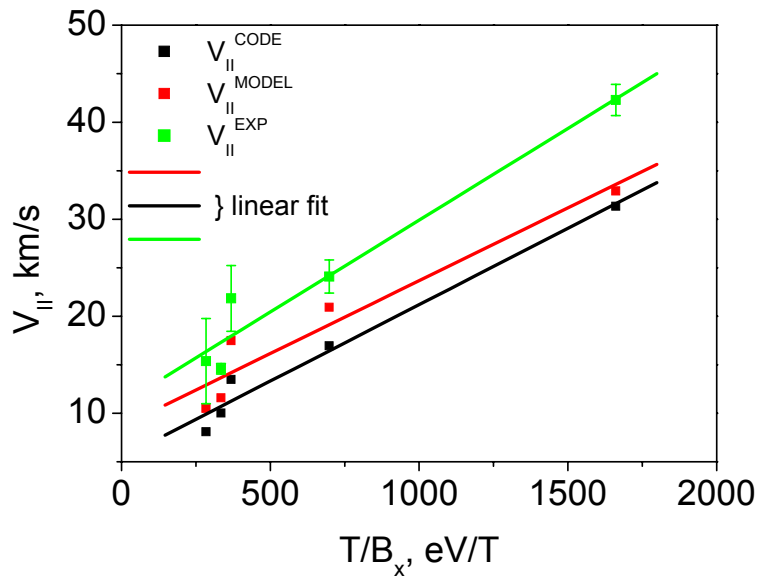


Fig.6. The absolute value of the parallel velocity at the reference point in the equatorial mid-plane 3 cm outside the separatrix as a function of the ratio of SOL temperature to poloidal magnetic field for all scenarios.

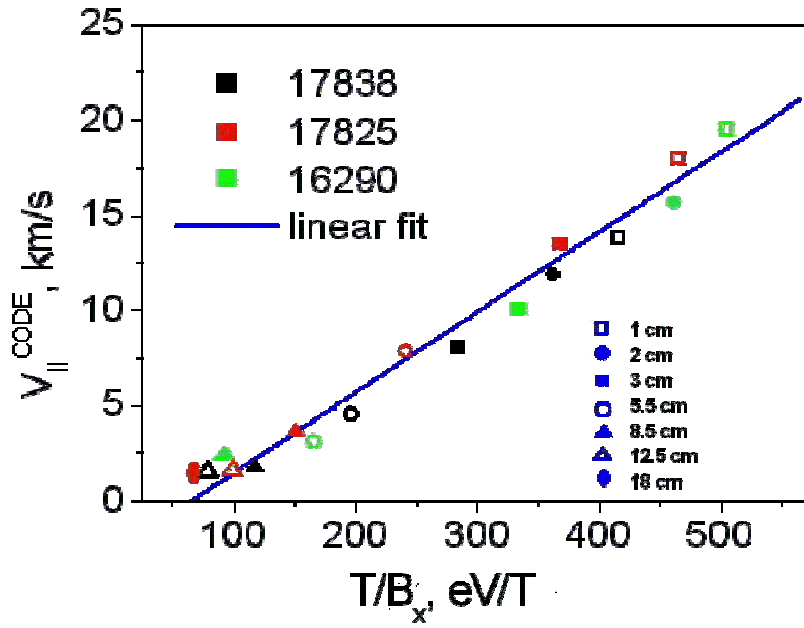


Fig.7. The absolute value of simulated parallel velocity V_{\parallel}^{CODE} as a function of of the ratio of ion temperature to poloidal magnetic field for scenarios №17838, №17825, №16290 .taken at the equatorial mid-plane from distance 1cm to 5 cm outside the separatrix. The coefficient A in Eq. (5) is 0.027.

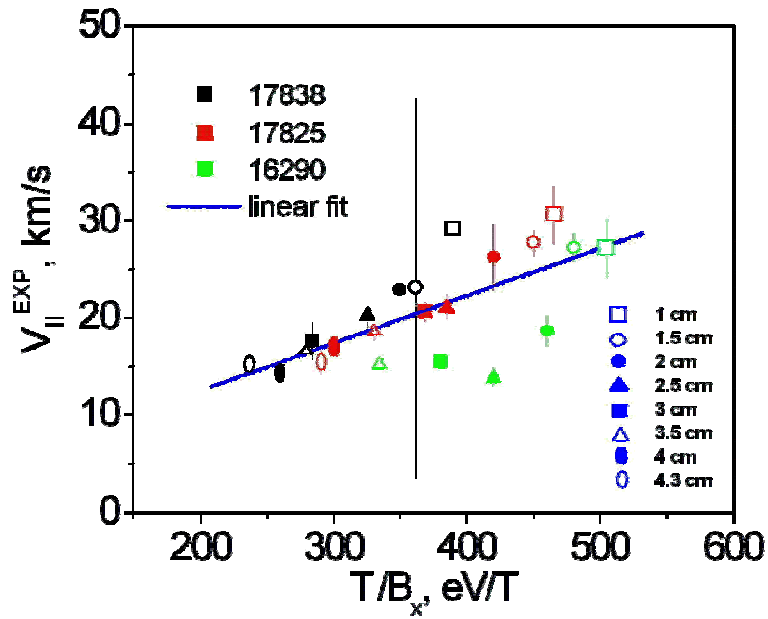


Fig. 8. The absolute value of the experimental parallel velocity V_{\parallel}^{EXP} as a function of of the ratio of code temperature (code values are used because the ion temperature profiles were not measured) to experimentally measured poloidal magnetic field for scenarios №17838, №17825, №16290 taken at the equatorial mid-plane from distance 1cm to 5 cm outside the separatrix. The coefficient A in Eq. (5) is 0,05.